Performance optimization of two-stage compressor system using transcritical R744

IOP Conf. Series: Materials Science and Engineering **604** (2019) 012034 doi:10.1088/1757-899X/604/1/012034

Performance optimization of two-stage compressor system using transcritical R744

S Elbel[1,2,3] **and P Hrnjak**[1,2]

[1] Air Conditioning and Refrigeration Center, University of Illinois at Urbana-Champaign, 1206 W. Green St., Urbana, IL 61801, USA
[2] Creative Thermal Solutions, Inc. (CTS), 2209 N. Willow Rd., Urbana, IL 61802, USA
[3] Author to whom correspondence should be addressed (elbel@illinois.edu)

Abstract. The use of transcritical R744 systems has become increasingly popular in recent years in a variety of different applications. For applications that span a wide temperature range between the heat source and heat sink, the use of two-stage compressor results in numerous advantages in terms of efficiency and compressor discharge temperature. This paper presents experimental data for a transcritical R744 compressor system operating at high heat rejection temperatures. A comprehensive system model was developed and validated with the experimental results. Based on this, the simulation tool was used to further optimize the system design specifically to accommodate the two-stage compression process. The optimum heat transfer area distribution has been determined to simultaneously ensure efficient intercooling at intermediate pressure and gas cooling at the high-pressure level. Simultaneously, the system was also optimized with respect to optimal intermediate pressure and the results show that for this particular system, the optimum intercooler pressure deviated substantially from the standard design approach that uses the geometric mean between suction and discharge pressures.

1. Introduction

CO_2 as a refrigerant (R744) is believed to be a promising replacement for HFC refrigerants due to its smaller environmental impact regarding the greenhouse potential. In addition, R744 provides larger volumetric cooling capacities than typical HFC refrigerants which could eventually yield higher cooling capacities for similarly sized systems [1]. For applications that span a wide temperature range between the heat source and heat sink, the use of two-stage compressor results in numerous advantages in terms of efficiency and compressor discharge temperature. The application studied in this paper is a packaged, unitary-type system as shown in figure 1, designed for military use in harsh environments. The system was retrofitted with transcritical R744 technology to provide 10.5 kW of air-conditioning at an outdoor temperature of 51.7°C and an indoor temperature of 32.2°C and 50% relative humidity.

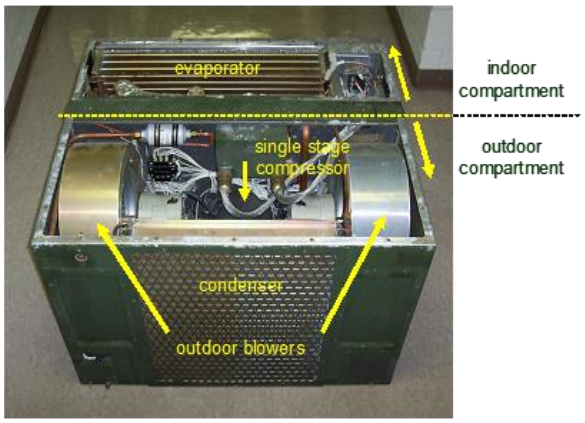

Figure 1. Unitary type air-conditioner with 10.5kW cooling capacity at 52°C/32°C - 50% RH.

2. System description

The transcritical R744 system was developed in a breadboard laboratory environment in which the air-side heat exchangers were mounted in dedicated wind tunnels. The schematic of the air-conditioning system is shown in figure 2. This system consists of a hermetic two-stage rolling piston compressor, an intercooler, a gas cooler, a suction line heat exchanger, a manual expansion valve, an evaporator and a suction accumulator.

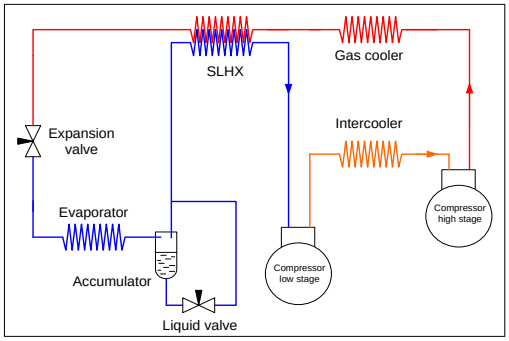

Figure 2. Transcritical R744 system consisting of two-stage compressor, gas cooler, suction line heat exchanger, expansion valve, evaporator, and accumulator with liquid valve.

All heat exchangers had an aluminum microchannel tube design. The microchannel tubes used for the gas cooler, the intercooler and the evaporator all had identical dimensions with six circular ports with a nominal hydraulic diameter of 0.76mm. The suction line heat exchanger had eleven square-shaped ports on the high-pressure side and 17 square-shaped ports on the low-pressure side with nominal side lengths of 1.29mm and 0.96mm, respectively. The gas cooler had four refrigerant slabs in series fed from a single inlet header. It was operated in a cross-counter flow arrangement. The intercooler had four parallel refrigerant slabs in cross-flow arrangement and the refrigerant inlet header acted as a distributor. The intercooler showed the biggest potential for improvement due to its cross-flow design. The cross-counter flow evaporator had two slabs in series, also having a single inlet header. The counter flow suction line heat exchanger was built in a sandwich design, where the low-pressure side consisted of three parallel tubes in two layers, whereas the high-pressure side had three parallel tubes in only one single layer. The compressor was of hermetic two-stage design housed in a prototype steel shell. The discharge flow of the low-stage compressor was used to internally cool the electric motor before it was sent to the intercooler. The displacements of the low and the high-side stages were 21.8cm^3 and 13.2cm^3, respectively. The compressor motor was rated at 3-phase 208V, 30A at 60Hz, corresponding to a

nominal speed of 3600min^{-1}. The target refrigerant mass flow rate at full capacity was designed to be 83g/s. The compressor did not have an external oil separator. The expansion valve used was a manual metering valve with an appropriate sensitivity in order to ensure repeatability of the valve settings in the transcritical tests. The accumulator used in the experiments was also of a prototype design and required an external liquid metering valve. Additional details regarding the setup can be found in [2]. Wind tunnel designs followed applicable industry standards [3]. Three independent energy balances were available to determine the cooling capacity of the system, namely on the air-side, the refrigerant-side, and through a calorimetric chamber balance. The experimental results typically agreed within 5% of each other.

3. Experimental results

The test matrix shown in table 1 specifies the conditions at which the system was investigated. For each outdoor temperature condition, several different high-side pressures were investigated by varying the opening of the expansion valve. The given outdoor air flow rate consisted of both the gas cooler and the intercooler air flows since both components were installed in the same duct. The face area ratio of the gas cooler to the intercooler equaled 3.053. The microchannel tube and the fin geometries of the gas cooler and the intercooler were identical. Therefore, the assumption of equal air velocities through both components was justified. In this case the volumetric air flow rates were split according to the same ratio as their face areas.

Table 1. Test matrix for experimental evaluation of transcritical R744 system.

	Outdoor temperature	Outdoor air flow rate	Indoor temperature	Indoor air flow rate	Relative humidity (indoor)	Compressor speed
	(°C)	(m^3/s)	(°C)	(m^3/s)	(%)	(min^{-1})
W1	32.2					
W2	43.3	0.8967	32.2	0.5663	50	3600
W3	51.7					

3.1. System performance

Figure 3 shows the experimental results of the system for the test conditions outlined in table 1.

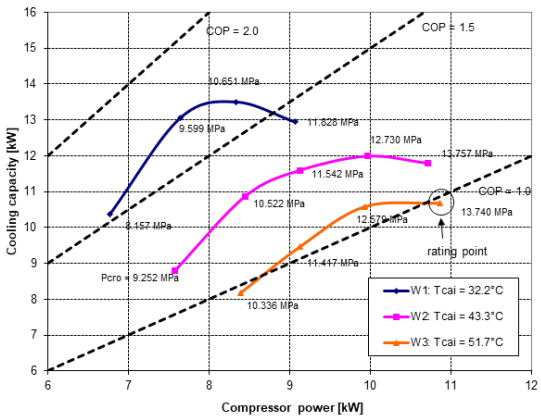

Figure 3. Experimental cooling capacities for conditions W1, W2, and W3 (label values indicate high-side pressures).

It can be seen that the maximum cooling capacity achieved was 13.5kW at condition W1, at an ambient outdoor air temperature of 32.2°C. W2 had an ambient outdoor air temperature of 43.3°C and a resulting maximum capacity of 12.0kW. At condition W3, the rating point, with an ambient outdoor air temperature of 51.7°C, the maximum cooling capacity was measured to be 10.7kW. The system had maximum COPs of 1.71, 1.29 and 1.07 at the conditions W1, W2, and W3, respectively. A Ph-diagram for the transcritical R744 system at condition W3 is shown in figure 4 for a variety of different high-side pressures.

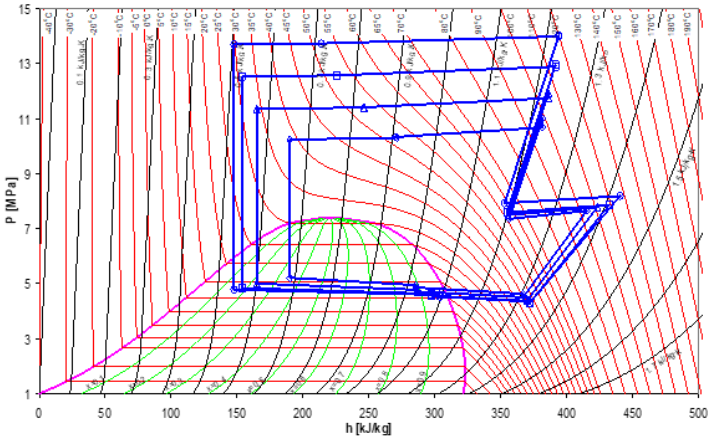

Figure 4. Ph-diagram for test condition W3 at different high-side pressures.

It can be seen that the compression ratio across the low-stage compressor is approximately constant while the compression ratio across the high-stage compressor increases significantly with increasing high-side pressures. This is due to the fact that the displacement volumes of the two-stage compressor are fixed and that the intermediate pressure level in the intercooler is mainly influenced by the ambient air conditions.

Since the refrigerant high-side pressure represents an additional degree of freedom in transcritical R744 systems, a system specific pressure control strategy was derived from the previous test points. As discussed in [4], [5], and [6], the system's high-side pressure has a significant influence on the performance, especially for pressures in the region above the critical point where the R744 isotherms are S-shaped. That means that at the same outdoor ambient condition (air temperature and flow rate) a small increase in high-side pressure results in a significant enthalpy change at the gas cooler exit, eventually increasing the enthalpy difference obtained in the evaporator. This increase of enthalpy difference in the evaporator results in a higher total compression ratio across the compressor and thus by an increased amount of work transfer to the system. This trade-off yields two performance maximizing high-side pressures for each condition. The high-side pressure at which the maximum COP is achieved is in general lower than the pressure at which the system has the highest cooling capacity. Based on the experimental data high-side pressure control equations were derived as shown in equation (1) and equation (2).

$$\text{Maximum Q: } P_{opt}\,[\text{MPa}] = 0.2137\; T_{gc,r,out}\,[^{o}\text{C}] + 3.0081 \tag{1}$$

$$\text{Maximum COP: } P_{opt}\,[\text{MPa}] = T_{gc,ref,out}\,[^{o}\text{C}] + 3.9917 \tag{2}$$

3.2. Compressor performance

The hermetic two-stage compressor was also analyzed. Figures 5a and 5b show the compressor efficiencies determined from the system tests. According to [7], the volumetric efficiency is defined by equation (3).

$$\eta_{volumetric} = \frac{\dot{m}_r v_r}{\omega V_d} \tag{3}$$

The compressor speed, even though not explicitly measured, was assumed to be 3600min^{-1}, corresponding to the 60Hz power supply used. It was also assumed that the compressor did not have any significant internal leakage between the compression stages. Thus, the mass flow rates through both compression stages were assumed to be equal. The volumetric efficiencies were calculated independently for the two compression stages and are shown in figure 5a.

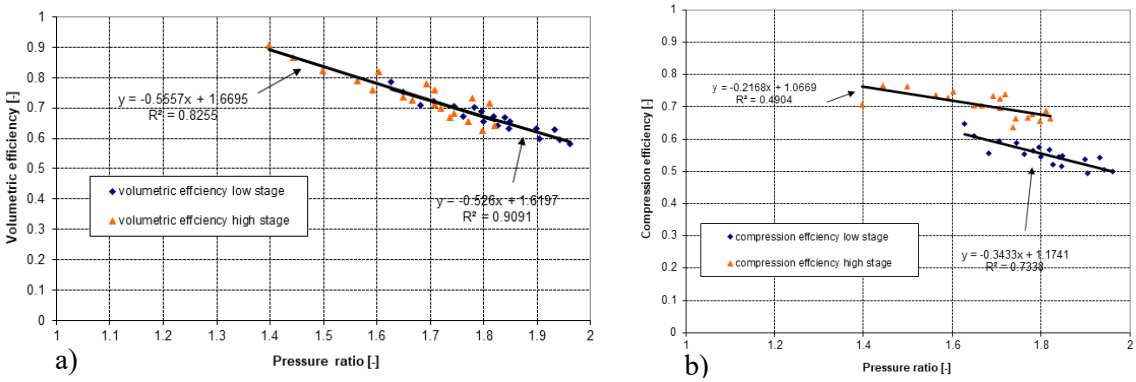

Figure 5. a) Volumetric and b) compression stage efficiencies of the R744 two-stage compressor.

According to [7], the compression efficiency is defined as the ratio of the isentropic compression enthalpy difference to the enthalpy difference required for the actual compression process, as shown in equation (4).

$$\eta_{compression} = \frac{\Delta h_{isentropic}}{\Delta h_{actual}} \tag{4}$$

Figure 5b shows the compression efficiencies for both stages plotted versus their compression ratios. For identical low-side and high-side pressure ratios, the resulting volumetric efficiencies of figure 5a of both stages were approximately equal. This is not the case for the compression efficiencies (figure 5b), which were consistently lower for the low-stage compression process. This is because the flow exiting the low-stage compressor is internally used to cool the electric motor driving the compressor before it is fed into the intercooler. That means that the temperature of the flow entering the high-stage compressor is artificially increased.

4. Description of simulation model

The R744 system was modeled with a finite element approach using EES software [8]. The model utilized a Newton-Raphson solver scheme. The steady-state model was originally developed by [9] and modified for this study. The two-stage compressor model was implemented based on experimentally determined correlations for the volumetric and compression efficiencies described earlier. The model structures of the gas cooler and the intercooler are similar even though the intercooler is of a cross flow design whereas the gas cooler is designed as a cross-counter flow heat exchanger. Because of the temperature glides, large numbers of finite elements were chosen for both the gas cooler and the intercooler. Each microchannel tube of each slab was divided into 40 equally sized elements. A UA-LMTD modeling approach was chosen to solve for the heat transfer rates of the individual elements. Emphasis was put on modeling the real structure of the heat exchanger in combination with validated correlations for air and refrigerant-side heat transfer coefficients and pressure drops. The model correlations used and a more detailed model description of the other components can be found in [2].

The simulated results for cooling capacity and COP was well within +/- 10% of experimental results for the majority of the data points. Figure 6 compares experimental and simulated results in a Ph-diagram.

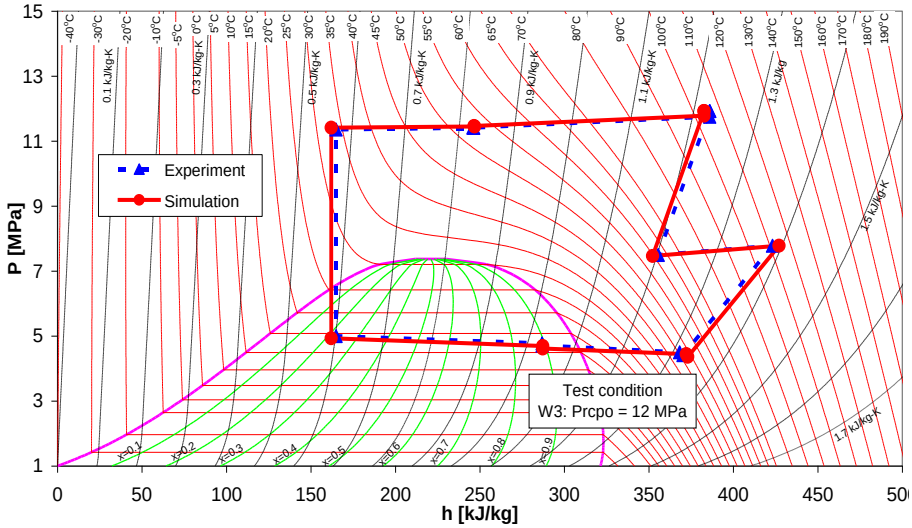

Figure 6. Comparison of experimental and simulated results in a Ph-diagram for test condition W3 at a high-side pressure of 12MPa.

5. System optimization

5.1. System performance

This section addresses the question of how the available outdoor coil space should be distributed among the gas cooler and the intercooler in order to maximize the system performance for otherwise unchanged conditions. The initial gas cooler / intercooler air-side area ratio as determined by the dimensions of the prototype heat exchangers was 3:1. In order to change this ratio, the intercooler face area was kept constant while parts of the gas cooler face area were covered with aluminum foil tape. Since the overall outdoor air flow rate was also kept constant, this method provided a way to vary the flow rate distribution between the two heat exchangers. For the test condition investigated, the influence of reduced gas cooler face area on the COP and the cooling capacity becomes significant if the area covered exceeds approximately 15% as shown in figure 7. Up to this value, the system performance is almost as high as in the case of an uncovered gas cooler. Once 20% or more of the heat exchanger are covered the performance drop becomes significant.

The simulation model was used to determine the performance maximizing air-side area distribution between the gas cooler and the intercooler. The analytical determination of the system COP took into account the power required to operate the indoor and outdoor fans. However, unlike in the experiments, the overall outdoor coil air-side face area, consisting of the gas cooler and the intercooler, was kept constant at the value prescribed by the dimensions of the prototype heat exchangers. Thus, when the system performance was simulated with reduced gas cooler air-side areas, the face area of the intercooler was increased proportionally at the same time in order to maintain identical overall outdoor coil dimensions.

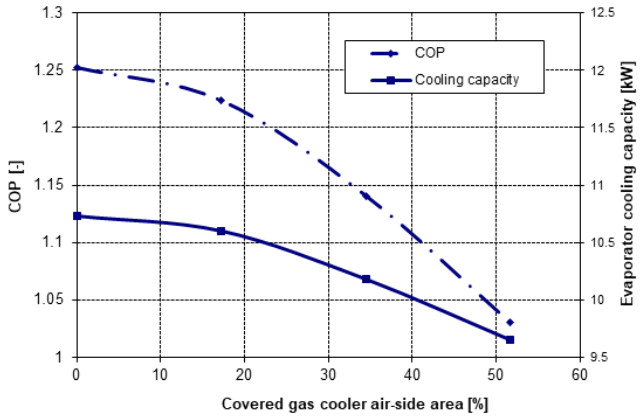

Figure 7. Experimental system performance for partially covered gas cooler air-side area as a function of the covered area at fixed indoor and outdoor air flow rates at condition W2.

Figure 8 presents the simulation results for gas cooler / intercooler air-side area ratios between 0.75 and 4. In accordance with the experimental results shown in figure 8, the system performance did not change significantly in the vicinity of the initial ratio, i.e. the COP and the evaporator cooling capacity were not reduced by much for cases in which the original gas cooler air-side area was covered by less than 15%. However, the cooling performance can be further increased if more of the available outdoor coil space is used for the gas cooler. At the same time, the system COP constantly drops. This is because the reduced gas cooler approach temperature eventually increases the refrigerant-side enthalpy difference across the evaporator and hence the cooling capacity. The COP decreases in this case, because of the reduced intercooler air-side area which results in increased work of the high-stage compressor.

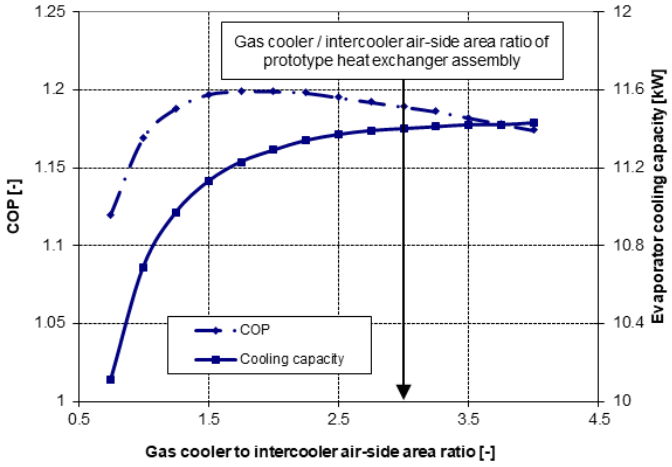

Figure 8. Simulated system performance for partially covered gas cooler air-side area as a function of the covered area at fixed indoor and outdoor air flow rates at condition W2.

For the opposite case with increased intercooler and proportionally reduced gas cooler face areas, the capacity drops while the COP increases. Figure 8 also shows that a maximum system COP is achieved for gas cooler / intercooler air-side area ratios between 1.5 and 2. For ratios smaller than that, the reduction in cooling capacity becomes over-proportional relative to the decreases in compression work, which explains the existence of the local COP maximum. Based on this analysis it appears that the initial choice to build the prototype gas cooler and intercooler with an air-side area ratio of 3 was reasonable.

However, in order to maximize the system COP, a smaller gas cooler / intercooler air-side area ratio should be considered.

5.2. System performance

Another important design parameter is the choice of the intermediate pressure level in the intercooler. The literature [10] suggests that there is a COP maximizing intercooler pressure for every desired overall compression ratio which is determined from the geometric mean of the corresponding low and high-side pressures, as shown in equation (5).

$$P_{intercooler,opt} = \sqrt{P_{low} \cdot P_{high}} \tag{5}$$

However, equation (5) can only be derived under several assumptions: thermally and calorically perfect gas, isentropic compression processes, identical suction temperatures at both compressor stages, and negligible refrigerant-side pressure drop in the intercooler. A numerical simulation modeling the compression processes was implemented in order to relax some of these crude assumptions. The model is based on a numerical integration of the compression work terms, which can be represented by areas underneath the compression paths in a pressure-specific volume diagram. The model takes real fluid properties of R744 rather than ideal gas behavior into account and it allows for non-isentropic compression processes.

For an ambient outdoor temperature of 43.3°C and compression efficiencies of 0.65, the influence of the high-stage discharge pressure on the work saving potential is illustrated in figure 9.

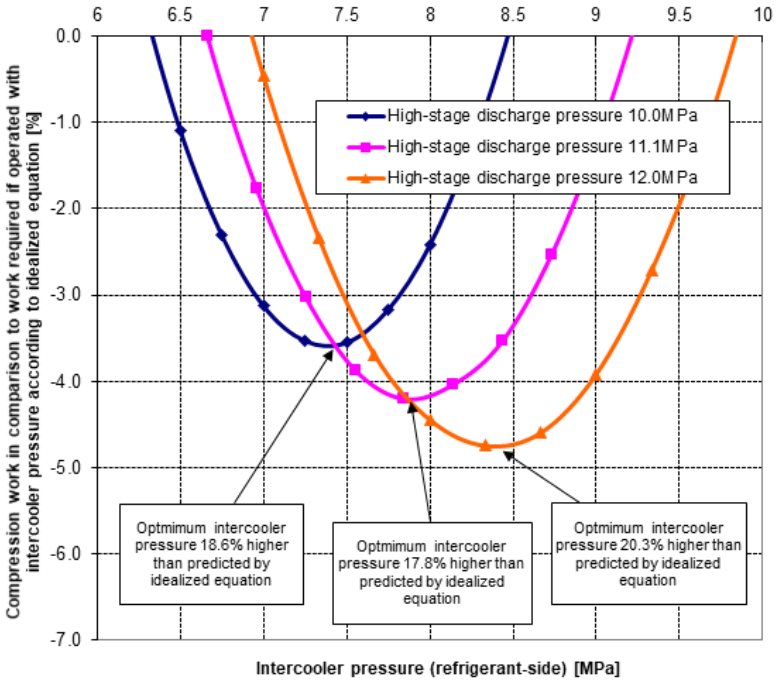

Figure 9. Work savings potential as a function of the intercooler pressure for various high-stage discharge pressures at condition W2.

For the lowest discharge pressure of 10.0MPa, the system requires 3.6% less compression work if operated at the optimum intercooler pressure in comparison to the value suggested by equation (5).

The optimum intercooler pressure in this case is 18.6% higher than the idealized value. For higher discharge pressures, the savings potential increases to 4.2% at 11.1MPa and 4.7% at 12.0MPa. Thus, the higher the discharge pressure the more important it becomes to operate the intercooler at its optimum

intermediate pressure in order to obtain the minimum work required. Maintaining the optimum intercooler pressure therefore improves the system COP especially at high evaporator loads, because such conditions typically require higher discharge pressures at the high-stage compressor.

The same type of analysis was carried out for different ambient outdoor temperatures as shown in figure 10. The high-stage discharge pressures were adjusted to match the COP-maximizing pressure according to the correlation given in equation (2). The compression efficiencies were again taken to be 0.65.

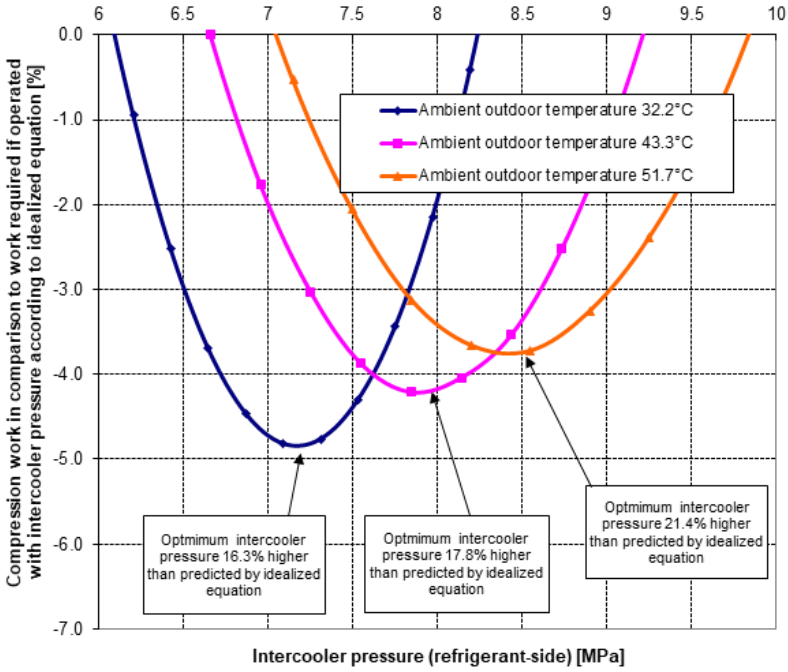

Figure 10. Work savings potential as a function of the intercooler pressure for various ambient outdoor temperatures.

For the ambient outdoor temperature range considered, the maximum possible work reduction occurs at 32.2°C where the system requires almost 5% less work when operated at its performance maximizing intermediate pressure in comparison to the value given by the idealized equation. As before, the numerically determined optimum intercooler pressures deviate significantly (16.3% to 21.4%) from the idealized pressure values suggested by equation (5). Thus, the possible work reductions become larger at lower ambient outdoor temperatures improving the system performance in particular at moderate ambient conditions.

6. Conclusions

A transcritical R744 system designed for air-conditioning at high ambient conditions was investigated experimentally and with the help of a simulation model. While the target capacity was achieved at the rating condition, the use of a two-stage compressor in combination with intercooler allows for further system improvements. While the choice of a gas cooler to intercooler area ratio of 3 appears to be a reasonable choice, higher COPs can be achieved with larger intercooler area at the expense of the size of the gas cooler. However, it should be noted that cooling capacity is affected in the opposite direction. Larger improvement potentials, with COP increases on the order of 5% were identified for optimized intermediate pressure ratios, showing that the commonly used geometric mean of high and low-side pressures should be understood merely as a general design guideline.

7. Nomenclature

Symbols		***Greek***	
COP	coefficient of performance (-)	Δ	difference
h	specific enthalpy (kJ/kg)	η	efficiency (-)
HFC	hydrofluorocarbon	ν	specific volume (m^3/kg)
LMTD	log. mean temperature difference (K)	ω	rotational speed (min^{-1})
m	mass flow rate (kg/s)		
Ṗ	pressure (kPa)	***Subscripts***	
Q	heat transfer rate (kW)	cai	air inlet outdoor coils
RH	relative humidity	d	displacement
SLHX	suction line heat exchanger	gc	gas cooler
T	temperature (°C)	max	maximum
UA	overall heat transfer coefficient times area (kW/K)	opt	optimum
V	volume (m^3)	out	outlet
W1-3	test conditions	r	refrigerant

8. References

[1] Connaghan M 2002 Experimental investigation of a breadboard model of a carbon dioxide U.S. army environmental control unit 9*th International Refrigeration and Conditioning Conference at Purdue (West Lafayette IN USA)* Paper R11-6

[2] Elbel S W and Hrnjak P S 2003 Experimental and analytical validation of new approaches to improve transcritical CO_2 wnvironmental control units *University of Illinois at Urbana-Champaign (Urbana IL USA)* ACRC Report CR-52

[3] ANSI/ASHRAE Standard 41.2-1987 (RA92) 1992 Standard methods for laboratory airflow measurement *American Society of Heating, Refrigeration and Air-Conditioning Engineers (Atlanta GA USA)*

[4] McEnaney R P, Yin J M, Bullard C W and Hrnjak P S 1999 An investigation of control-related issues in transcritical R744 and subcritical R134a mobile air-conditioning systems *University of Illinois at Urbana-Champaign (Urbana IL USA)* ACRC Report CR-19

[5] Elbel S 2000 Erste Regelungskonzepte eines Fahrzeugsystems für hohen thermischen Insassenkomfort, *Diploma Thesis at DaimlerChrysler AG Stuttgart (Stuttgart Germany)*

[6] Inokuty H 1928 Graphical method of finding compression pressure of CO_2 refrigerating machine for maximum coefficient of performance *Proc. 5th Int. Congress of Refrigeration (Rome Italy)* 185-192

[7] ASHRAE Handbook 2000 HVAC Systems and Equipment *American Society of Heating, Refrigeration and Air-Conditioning Engineers (Atlanta GA USA)* SI ed. chapter 34

[8] EES 2019 *Engineering Equation Solver – Academic Version* F-Chart Software *(Madison WI USA)*

[9] Yin J M 2001 MAC2R744 system model description *University of Illinois at Urbana*-Champaign *(Urbana IL USA*) Internal ACRC Document

[10] Moran M J and Shapiro H N 2000 *Fundamentals of engineering thermodynamics* Wiley & Sons *(New York NY USA)*, 4th ed 463-464

Acknowledgements

The authors would like to thank the member companies of the Air Conditioning and Refrigeration Center at the University of Illinois at Urbana-Champaign for their financial and technical support and Creative Thermal Solutions, Inc. (CTS) for their technical support.